Dentomaxillofacial Radiology (2017) 46, 20160296

birpublications.org/dmfr

RESEARCH ARTICLE

Imaging evaluating of the implant/bone interface—an *in vitro* radiographic study

[1]Michele M Vidor, [2]Gabriela S Liedke, [1]Mariana B Vizzotto, [1]Heraldo L D da Silveira, [1]Priscila F da Silveira, [3,4]Cristiano W Araujo and [1]Heloisa E D da Silveira

[1]Department of Surgery and Orthopedics, School of Dentistry, Federal University of Rio Grande do Sul (UFRGS), Porto Alegre, Brazil; [2]Department of Stomatology, School of Dentistry, Federal University of Santa Maria (UFSM), Santa Maria, Brazil; [3]Institute of Informatics, Universidade Federal do Rio Grande do Sul (UFRGS), Porto Alegre, Brazil; [4]Viewbox Software, Porto Alegre, Brazil

Objectives: To analyze the diagnostic accuracy of conventional and digital radiographic images and the impact of digital filters in evaluating the bone–implant interface.
Methods: Titanium implants were inserted into 74 fresh bovine ribs blocks, 37 fitting tight to the bone walls (simulating the existence of osseointegration) and 37 with a gap of 0.125 mm (simulating a failure in the osseointegration process). Periapical radiographs were taken with conventional film and two phosphor plate systems [VistaScan® (Dürr Dental, Bietigheim-Bissingen, Germany) and Express® (Instrumentarium, Tuusula, Finland)]. Digital radiographs were investigated with and without enhancement filters. Three blinded examiners assessed the images for the presence of juxtaposition in the bone–implant interface using a five-point Likert scale. Sensitivity, specificity and the area under the receiver-operating characteristic curve (AUC) and its 95% confidence interval (CI) were calculated for each variable. Intraexaminer and interexaminer agreements were analyzed using Kendall's concordance test.
Results: Intraexaminer and interexaminer agreements were >0.80 for both digital and conventional images. Conventional radiographs (AUC = 0.963/CI = 0.891 to 0.993) and digital images with high enhancement filters such as Caries2 (AUC = 0.964/CI = 0.892 to 0.993), Endo (AUC = 0.952/CI = 0.875 to 0.988) and Sharpen3 (AUC = 0.894/CI = 0.801 to 0.954) showed the greatest accuracy for evaluating the bone–implant interface. Original images from both digital systems and the further enhancement filters tested showed low sensitivity for the diagnosis task tested.
Conclusions: Conventional radiographs or digital radiographs with high-pass filters could help enhance diagnosis on implant–bone interface.
Dentomaxillofacial Radiology (2017) **46**, 20160296. doi: 10.1259/dmfr.20160296

Cite this article as: Vidor MM, Liedke GS, Vizzotto MB, da Silveira HLD, da Silveira PF, Araujo CW, et al. Imaging evaluating of the implant/bone interface—an *in vitro* radiographic study. *Dentomaxillofac Radiol* 2017; **46**: 20160296.

Introduction

Periapical radiographs are recommended for post-operative evaluation of dental implants in the absence of clinical signs or symptoms, contributing to the early diagnosis of associated pathologies, such as the presence of peri-implant radiolucency, and a quantitative analysis of bone loss adjacent to the implant.[1,2] The introduction of digital radiology brought some advantages to the dentist and patients, such as a decrease in the time of the examination and the elimination of the dark room and chemical use. The possibility of image processing is an important advantage, taking into consideration that the use of specific filters contributes to the examination accuracy.[3,4] However, studies have also shown that digital imaging processing used to enhance

Correspondence to: Dr Gabriela Salatino Liedke. E-mail: gabriela.liedke@ufsm.br
Received 19 July 2016; revised 9 February 2017; accepted 13 February 2017

the visualization of some structures may generate artefacts which have a harmful impact and could jeopardize the evaluation.[5–8]

Digital radiographic images are based on a numerical matrix, where each element of this matrix is composed of one fundamental element: the pixel (picture element). When processing techniques are employed, the matrix is modified through a wide range of algorithms that execute mathematical transformations, changing the pixel values. Therefore, it is possible to, for example, enhance a particular structure, reduce noise or extract relevant attributes or information. The Fourier transform provides a mean of decomposing an image in the multiple frequencies composing it. The difference of the Fourier transform among pre- and post-filtered images can be used to analyze which frequencies are enhanced or diminished in the image when passed through a filter.[9,10]

The choice of the digital image processing used depends on the structure being evaluated. Thus, the knowledge of how the processing filters modify the digital matrix and its impact on the examiner diagnosis become important in diverse clinical situations. Regarding dental implants, there are no studies either comparing conventional and digital radiographs or evaluating the effect of processing filters in the bone–implant interface diagnosis. Therefore, the objective of this *in vitro* study was to analyze the diagnostic accuracy of conventional and digital radiographic images and the impact of processing filters used in digital radiographs, for the evaluation of bone–implant interface, to suggest an adequate protocol for radiographic evaluation in clinical situations.

Methods and materials

Sample preparation

The present study was approved by the Research and Ethics Committees of the Federal University of Rio Grande do Sul (no 26,464). Sample calculation was performed using Winpepi [Abramson JH (PEPI-for-Windows): computer programs for epidemiologists (Epidemiologic Perspectives & Innovations 2004)], considering the capability of radiography in detecting bone–implant interface juxtaposition. Assuming equal chances for both situations (with and without juxtaposition of the implant to the bone tissue), significance level of 5%, and power of the test of 80%, a total of 74 radiographic images for each analyzed group were needed.

74 bovine fresh rib blocks were sectioned and used to individually allocate the implants. 37 titanium implants [Titamax TI Cortical®; Neodent, Curitiba, Brazil (4.1 mm × 3.75 mm × 9.0 mm)], used twice, were inserted in the middle region of the rib blocks. The sample was divided into test group (TG) ($n = 37$) and control group (CG) ($n = 37$), depending on the implant–bone wall interface.

On CG, the perforations were performed according to the recommended sequence of drills specified by the manufacturer, in which the 3.0-mm diameter drill is the last one used before the insertion of a 3.75-mm diameter implant. The implant was inserted constricted to the bone walls, until a primary stability at 45 N cm was achieved, resulting in a perfect juxtaposition of bone–implant interface. To obtain an adequate setting of the implant platform to the bone, a counter sink drill was used.

On TG, the perforations were made using the same sequence used for the CG, adding the 4.0-mm diameter drill. Thus, a 3.75-mm diameter implant was installed in perforations of 4.0-mm diameter, creating a gap of 0.125 mm around the implant body. A counter sink drill was used and guaranteed that the implant platform was positioned stable at the bone level, avoiding any movement of the implant body inside the perforation.

Radiographic image acquisition

Each rib block with the inserted implant was positioned and stabilized on a flat surface for radiographic acquisition. A positioning device was used to ensure parallelism between the implant and the receptor. A perpendicular focus-receptor incidence was used, with a 30-cm focus-receptor distance. Each implant was imaged with three radiographic systems: the conventional radiographic film Kodak Insight no 2 (Eastman Kodak, Rochester, NY), storage phosphor plate systems VistaScan® (Dürr Dental, Bietigheim-Bissingen, Germany) and Express®(Instrumentarium, Tuusula, Finland) (Table 1). The same intraoral machine [Spectre 70X; (Dabi Atlante, Ribeirão Preto/São Paulo, Brazil) (127 V, 8 A, 50/60 Hz)] with exposure time of 0.4 s was used. The soft tissues were maintained on the ribs to attenuate the X-rays.

Conventional radiographs were developed in an automatic processor (Model 9000; DENT-X, Elmsford, NY) and stored on cards coded for the evaluated outcome. The processing of phosphor plates took place in the manufacturer system scanner. Digital radiographs were enhanced with the high-pass filters available in the software DBSWin (Durr Dental AG, Bietigheim-Bissingen, Germany) and CLINIVIEW™ (Instrumentarium, Tuusula, Finland), exported and saved in tagged image file format, as shown in Table 1 and illustrated in Figure 1.

Imaging evaluation

Three oral and maxillofacial radiologists assessed the images to evaluate the bone–implant interface. A five-point Likert scale was used, with the following formation: (1) definitely there is a juxtaposition of bone–implant interface; (2) probably there is juxtaposition; (3) uncertain; (4) probably there is no juxtaposition; and (5) definitely there is no juxtaposition of bone–implant. Before the study, the examiners received a presentation lecture to become familiar with the outcome evaluated, the filters and the scoring scale.

Conventional radiographs were evaluated on a light box with black masking, and with the use of a magnifying glass, in a room with reduced lighting. Digital radiographs

were visualized on a flat-screen monitor [(LG Flatron—E2250; Lg electronics, Manaus/Amazonas, Brazil), using the Image Viewer from Windows (Microsoft®, Redmond, WA)], in a room with controlled lighting; the zoom tool was available. Digital images were presented individually and coded, in a blinded and random sequence, without any information about the filters. After a 4-week period, the interpretation of 20% of the sample was repeated to evaluate intraexaminer and interexaminer agreement.

Data analysis

Statistical analysis was performed with the software SPSS® (IBM Corp., New York, NY; formerly SPSS Inc., Chicago, IL) and Microsoft® Office Excel® 2010 (Microsoft, Redmond, WA). Significance was set at 0.05 or less.

Kendall's coefficient of concordance (W) was used to evaluate intraexaminer and interexaminer agreement, considering all five scores on Likert scale. The mode used for subsequent evaluations among the examiner scores was [(score Ex1) − (score Ex2) − (score Ex3)].

The diagnostic tests (sensitivity and specificity) and the area under the receiver-operating characteristic curve (AUC) with its respective 95% confidence interval were calculated for each studied variable: image acquisition system (Conventional, VistaScan and Express) and filter. The DeLong method was used to compare the AUCs, evaluating the impact of image acquisition system and filter. Each of the digital systems were assessed independently for the comparison among the processing filters and with the conventional radiography.

The impact of each processing filter on the digital images was evaluated using a three-dimensional (3D) graph of the magnitude spectrum of the Fourier transform [Python (www.python.org) programming language in conjunction with OpenCv library (opencv.org)]. The Fourier transform changes the image from the spatial to the frequency domain, allowing an objective evaluation of the filter action in relation to the bone–implant interface. Mathematically, the image is a function, $z = f(x, y)$, in which x and y define the frequency. In the frequency spectrum, which can be shown as a 3D graph, each frequency participation percentage is represented by z. The comparison among the 3D graphs allows a better comprehension of which frequencies are overlapped in the original signal and how much of this frequency is present in the image.[9,11] Conventional radiographs were scanned into tagged image file format digital format using an Astra 2400S scanner (UMAX, Dallas, TX) and resolution of 1200 dpi, so that the images could also be evaluated by this methodology. Digital images and digitized conventional radiographs were sectioned; so, only the body of the implants was used, and the graphs were influenced by neither the cortical bone nor the air space.

Results

Each examiner evaluated 74 conventional and 814 digital radiographs. Table 2 shows the distribution of the examiner answers among the five available scores in the Likert scale.

Intraexaminer and interexaminer concordances are shown in Table 3. Intraexaminer agreement was always >0.90 for both digital and conventional images. Interexaminer agreements were 0.826 and 0.904 for digital and conventional images, respectively.

Table 4 shows the values of sensitivity, specificity and AUC with its respective 95% confidence interval for each variable. The greatest sensitivity and specificity values were associated with conventional radiographs and digital images from VistaScan system with high-pass filters using strong matrix penetrance. Original digital images, those processed with high-pass filters with low matrix penetrance from the VistaScan system, and all evaluated filters from the Express system showed low sensitivity for the diagnosis of failure in bone–implant interface (that is, they were related with a high number of false-negative diagnoses).

The DeLong method showed equivalence between conventional radiographs and digital images processed with high-pass filters (Caries2, Endo and Sharpen3). The remaining studied filters showed statistically significant differences when compared with conventional radiography ($p < 0.05$). In relation to VistaScan system, the filters Perio and Fine did not present a statistically significant difference when compared with the filter Endo ($p < 0.05$). The original digital images from VistaScan were statistically significantly different from all the others, except Caries1. In relation to Express system, the original images and Sharpen4 showed a statistically significant difference when compared with Sharpen3 filter.

Table 5 depicts the changes in low- and high-frequency components seen in an image after it was post-processed by each selected filter. It is possible to see that each filter behaved differently. Some high-pass filters led to the increase of only high frequencies, without diminishing the participation of low frequencies in the image, when compared with the original image (*i.e.* Sharpen 2, Sharpen 3 and Sharpen 4). For some other high-pass filters, both the decrease in the participation of low frequencies and, at the same time, the increase in the participation of high frequencies, was observed in comparison with the original image. Those latter filters originated images that presented better performance in the diagnostic tests.

Figure 1 shows the 3D graphs illustrating the Fourier transform for each image evaluated. The graph should be interpreted in such a way that its centre represents higher frequencies, decreasing to low frequencies on the outlines. The colours represent the participation (intensity) of a determined frequency in the image composition (dark blue represents the lowest value; light blue, medium–low value; green, medium–high value; and yellow and red, the highest frequency values). Image loses sharpness if high values (red or yellow) are close to the outlines or if there is no significant contribution from high-frequency components. Analyzing the

Table 1 Radiographic systems and filters

System	*Kodak*	*VistaScan*®	*Express*®
Type of receptor	Insight film no 2	Phosphor plate	Phosphor plate
Commercial brand	Eastman Kodak (Rochester, NY)	Dürr Dental (Bietigheim-Bissingen, Germany)	Instrumentarium (Tuusula, Finland)
Evaluated Images	–	Original	Original
		Fine	Sharpen 1
		Caries 1	Sharpen 2
		Caries 2	Sharpen 3
		Endo	Sharpen 4
		Perio	

graphs, it is possible to observe that in conventional radiographs, there is a proportional distribution of high and low frequencies. Regarding the digital images that showed the best performance (Caries2, Endo and Sharpen3), the filters privileged the participation of high frequencies, observed in the central area of the graph, which is seen to be higher and broader. It is important to point out that the graphs can be compared only inside each system owing to their differences in image receptors.

Discussion

Specific filters for digital radiograph processing can contribute to image evaluation and diagnosis when correctly indicated.[8,12–14] The present research investigated the impact of filter for bone–implant interface evaluation, as radiographs are indicated for post-operative evaluation of dental implants.[1] Enhanced images are preferred among dentists who evaluate digital radiographs.[3,4,15] The selected filters may produce only slight differences among the images, so a binary (yes/no) answer might not have been enough to reveal small differences among them. Therefore, a five-point Likert scale was adopted, allowing a better understanding of the behaviour of each digital filter, according to the confidence level of the answer given by the examiners.[16] Besides, the Likert scale adopted allowed the observer to express doubtful estimations.

Original digital radiographs and those processed with a high-pass filter with low matrix penetrance were more related to a diagnosis of bone–implant juxtaposition (Score "1"), suggesting that such images could confound the examiner and increase false-negative diagnosis. In contrast, increasing the penetrance of the high-pass filter increased the diagnosis of failure in bone–implant interface (Score "5") and, especially, that of examiner doubt (Score "3"). The concern regarding the use of high-pass filters and misinterpretation of digital images had been reported in the literature.[5,8] For bone–implant interface, Express digital system, especially Sharpen4 filter, was more related to increased examiner doubt (Score "3", $n = 32$), while conventional

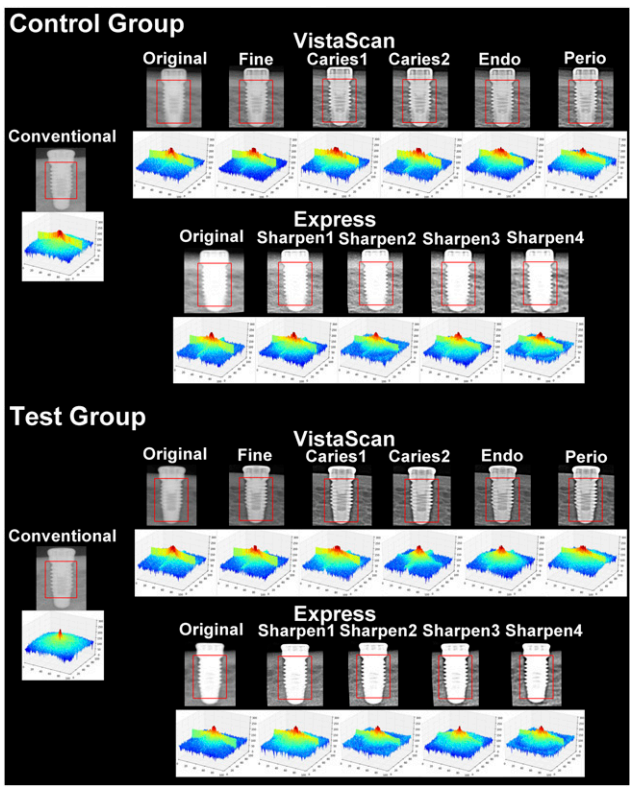

Figure 1 A representative close-up of radiographs from each acquisition system and filter and the relative three-dimensional (3D) Fourier transform graphs in the control and test groups. The squares represent the selection used for the 3D graph analysis.

Table 2 Frequency (mode) of score answers among the three examiners for each acquisition system and filter ($n = 74$)

		Likert scale				
System	*Filter*	*1*	*2*	*3*	*4*	*5*
Conv	–	35	9	3	2	25
VistaScan®	Org	51	3	7	3	10
	Fin	39	1	11	6	17
	Ca1	10	13	8	13	30
	Ca2	10	18	12	12	22
	Endo	25	13	5	9	22
	Perio	7	17	10	13	27
Express®	Org	57	3	6	1	7
	Sh1	48	7	5	2	12
	Sh2	29	20	8	8	9
	Sh3	18	18	26	7	5
	Sh4	6	15	32	12	9

Ca1, Caries1; Ca2, Caries2; Conv, Conventional; Fin, Fine; Org, Original; Sh1, Sharpen1; Sh2, Sharpen2; Sh3, Sharpen3; Sh4, Sharpen4.

Table 3 Intraexaminer and interexaminer agreement for each image acquisition system

	Intraexaminer			
System	*Examiner 1*	*Examiner 2*	*Examiner 3*	*Interexaminer*
Conventional	0.928	0.904	0.966	0.904
Digital	0.954	0.943	0.942	0.826

radiographs generated more confidence during evaluations (Score "3", $n = 3$).

Sensitivity, specificity and accuracy tests should be considered when deciding for a diagnostic test.[16] Higher values for sensitivity, specificity and AUC were obtained with conventional radiographs, and digital images from VistaScan system were processed with a strong penetrance high-pass filter. On the contrary, original digital images, those with low-penetrance high-pass filter from VistaScan system and all images from Express system presented lower sensitivity for the diagnosis of failure in bone–implant interface. Clinically, this result represents a risk of non-detecting failures in the osseointegration process. Such differences among the evaluated images could be related to the imaging method, since intraexaminer and interexaminer agreements were high.

The act of selecting one or another filter is often subjective to and dependent on the digital system used. Therefore, the user might use one filter to create a successful or unsuccessful image, in spite of assessing the real condition. Enhancement filters, or high-pass filters, are the preferred ones among dentists who evaluate digital radiographs,[3,4,15] and, for this reason, those filters were the target in this investigation. In general, high-pass filters emphasize image borders, sharpening high-contrast differences in the image, and attenuating low frequencies (that is, the blur is removed). The available high-pass filters are named according to the anatomic region the filter is supposed to enhance (VistaScan system, *e.g.* "Caries", for the enamel and dental–enamel junction; "Endo", for the root canal system; and "Perio", for the bone crest and periodontal gap) and by the degree of filter strength (Express system, *e.g.* Sharpen1, Sharpen2; VistaScan system, *e.g.* "Caries1", "Caries2"). However, for trade purposes, the algorithms used to mathematically modify a digital image vary depending on the software and are rarely provided by the manufacturers, making a direct comparison among the filters difficult. Therefore, the images were also evaluated based on the Fourier transform difference. The frequency spectre does not have information regarding the filter itself, but the comparison among the spectres provides qualitative and quantitative information that can be used to analyze the mathematical operation achieved with the filters. The graphs regarding conventional radiographs show symmetry between blurriness and sharpness, representing the equilibrium in high- and low-frequency participations. Meanwhile, the graphs of digital images that had better diagnostic performances show a greater participation of high frequencies, perceived through the high and broad centre, seen as the increasing of image sharpness due to the use of high-pass filters. To eliminate noise, high-frequency components can be removed or the intensity of the low-frequency components can be increased by using low-pass filters, generating more homogeneous and softer images.[13] The enhancement of structure boundaries can be achieved by decreasing the intensity of the low-frequency components or by increasing the high-frequency components (high-pass filters), generating images with more accentuated characteristics.[10,13,15] However, depending on the structure being evaluated, and the filter being used, noise may be over-introduced in the image, impairing the diagnosis, especially when metal components are present.[5,8,17]

Some studies have also evaluated the impact of digital image processing on the diagnosis adjacent to metallic materials. The detection of a misfit in metal-restored teeth showed higher accuracy for conventional radiographs or original digital images; specifically, high enhancement filter should be avoided.[8] For measuring peri-implant bone level, original digital images, fine and

Table 4 Mean sensitivity, specificity and area under receiver-operating characteristic curve (AUC) [and confidence interval (CI) of 95%] among the three examiners for conventional and digital radiographs and filters

System	*Filter*	*Sensibility*	*Specificity*	*AUC (95% CI)*
Conv	–	0.730	1.000	0.963 (0.891 a 0.993)^{A}
VistaScan	Org	0.351	1.000	0.771 (0,659 a 0.861)^{D}
	Fin	0.568	0.946	0.872 (0.774 a 0.938)^{BCD}
	Ca1	0.838	0.676	0.782 (0.671 a 0.870)^{CD}
	Ca2	0.838	0.919	0.964 (0.892 a 0.993)^{A}
	Endo	0.784	0.946	0.952 (0.875 a 0.988)^{AB}
	Perio	0.892	0.811	0.858 (0.757 a 0.928)^{BCD}
Express	Org	0.216	1.000	0.708 (0.591 a 0.808)^{CD}
	Sh1	0.378	1.000	0.851 (0.750 a 0.923)^{BD}
	Sh2	0.405	0.946	0.849 (0.747 a 0.921)^{BD}
	Sh3	0.297	0.973	0.894 (0.801 a 0.954)^{AB}
	Sh4	0.405	0.838	0.737 (0.622 a 0.833)^{D}

Ca1, Caries1; Ca2, Caries2; Conv, Conventional; Fin, Fine; Org, Original; Sh1, Sharpen1; Sh2, Sharpen2; Sh3, Sharpen3; Sh4, Sharpen4.
AUC followed by different letters indicate statistical difference at $p < 0.05$.

Table 5 Components reduced and increased in the image (considering the participation of low and high frequency in the image) after the post-processing of selected filters, as revealed by the Fourier transform

Filter	*Component size reduced (low frequencies)*	*Component size increased (high frequencies)*
Caries 1	100–66%	1–66%
Caries 2	100–66%	1–66%
Endo	100–80%	1–80%
Fine	100–50%	1–50%
Perio	100–90%	1–90%
Sharpen 1	100–60%	1–60%
Sharpen 2		1–15%
Sharpen 3		1–7%
Sharpen 4		1–7%

emboss filters are suggested, while high-pass filters should not be used.[13] It is important to mention that the former study[13] has analyzed some of the available filters in one digital system (DBSWIN software) and that none of them were specifically developed for implant evaluation. Thus, the lack of specific filters requires that several post-processed images be tested for the same diagnostic task. In the present study, conventional radiographs presented the highest accuracy for the diagnosis of bone–implant interface. Furthermore, some high-pass filters (such as Caries2 and Endo) showed performance similar to conventional radiographs and are also indicated. The difference for the behaviour of such high-pass filters adjacent to metal materials could be related to the density of nearby structures with which the X-ray photons interact. When the bone–implant interface was the target of investigation, the difference in density between the metal and the bone tissue was not as significant as that between the metal and the adjacent air, as the two studies mentioned above.

Dave et al[18] also examined the diagnosis of bone defects in the bone–implant interface using digital radiography and CT, obtaining an AUC of 1 (the highest possible value) with the digital radiographs. The accuracy found in the present study varied from 0.964 (VistaScan system, Caries2 filter) to 0.708 (Express system, original image). However, some important differences should be mentioned. The former study[18] assessed gaps of 0.35-mm and 0.675-mm size, substantially larger than the ones in this investigation (0.125 mm). Furthermore, the authors did not comment on the use of processing filters that, as demonstrated, may interfere in the peri-implant evaluation.

The present study was based on an *in vitro* model, since the same implant needed to be imaged by several acquisition systems using ionizing radiation, making the participation of patients impossible. Bovine ribs with muscle tissue were chosen as the site for the implants, as the density of this region resembles that of the human mandibular bone tissue; besides, its use has already been documented.[18] One might suggest that the complexity of the biologic process involved in the osseointegration process cannot be reproduced *in vitro*. However, the present study is focused on the radiographic appearance of "juxtaposition" or "absence of juxtaposition" of bone–implant interface. A 3.75-mm-diameter implant was installed in perforations with 3.0-mm (CG) or 4.0-mm (TG) diameter. Thus, at the radiographic examination, there were two possible situations: either the implant would be in a close contact to the bone walls (CG), representing the osseointegration process, or a thin radiolucent line would be seen (TG), resulting in the absence of juxtaposition of bone–implant interface in the radiography, similar to the image of a failure of the osseointegration process. Moreover, the apical third of the chosen implants and the perforation drills had the same macroscopic design, allowing better setting and blinding of the examiners during the evaluations.

Conclusions

The results from this *in vitro* study showed that radiographic evaluation of bone–implant interface is influenced by the radiographic system and the processing filter employed. According to the results from the present study, conventional radiographs or digital images with application of high-pass filters such as "Caries2" and "Endo" could help enhance diagnosis on implant–bone interface on intraoral radiographs.

References

1. Tyndall DA, Price JB, Tetradis S, Ganz SD, Hildebolt C, Scarfe WC; American Academy of Oral and Maxillofacial Radiology. Position statement of the American Academy of Oral and Maxillofacial Radiology on selection criteria for the use of radiology in dental implantology with emphasis on cone beam computed tomography. *Oral Surg Oral Med Oral Pathol Oral Radiol* 2012; **113**: 817–26. doi: https://doi.org/10.1016/j.oooo.2012.03.005
2. Reddy MS, Wang IC. Radiographic determinants of implant performance. *Adv Dent Res* 1999; **13**: 136–45. doi: https://doi.org/10.1177/08959374990130010301
3. Yalcinkaya S, Kunzel A, Willers R, Thoms M, Becker J. Subjective image quality of digitally filtered radiographs acquired by the Durr VistaScan system compared with conventional radiographs. *Oral Surg Oral Med Oral Pathol Oral Radiol Endod* 2006; **101**: 643–51. doi: https://doi.org/10.1016/j.tripleo.2005.08.003
4. Wenzel A, Moystad A. Work flow with digital intraoral radiography: a systematic review. *Acta Odontol Scand* 2010; **68**: 106–14. doi: https://doi.org/10.3109/00016350903514426
5. Brettle D, Carmichael F. The impact of digital image processing artefacts mimicking pathological features associated with restorations. *Br Dent J* 2011; **211**: 167–70. doi: https://doi.org/10.1038/sj.bdj.2011.676
6. Tan TH, Boothroyd AE. Uberschwinger artefact in computed radiographs. *Br J Radiol* 1997; **70**: 431. doi: https://doi.org/10.1259/bjr.70.832.9166087
7. Oestmann JW, Prokop M, Schaefer CM, Galanski M. Hardware and software artifacts in storage phosphor radiography. *Radiographics* 1991; **11**: 795–805. doi: https://doi.org/10.1148/radiographics.11.5.1947316
8. Liedke GS, Spin-Neto R, Vizzotto MB, Da Silveira PF, Silveira HE, Wenzel A. Diagnostic accuracy of conventional and digital radiography for detecting misfit between the tooth and restoration in metal-restored teeth. *J Prosthet Dent* 2015; **113**: 39–47. doi: https://doi.org/10.1016/j.prosdent.2014.08.003
9. Gonzalez R, Woods R. *Digital image processing*. New York: Prentice Hall; 2001. doi: https://doi.org/10.1117/1.3115362
10. Rangayyan R. Enhancement. In: Rangayyan R (ed). *Handbook of medical imaging: processing and analysis*. New York: Academic Press; 2000. pp. 3–65. doi: https://doi.org/10.1016/b978-012077790-7/50003-5
11. Watt A, Policarpo F. *The computer image*. New York: Addisson-Wisley; 1998.
12. Haiter-Neto F, Casanova MS, Frydenberg M, Wenzel A. Task-specific enhancement filters in storage phosphor images from the VistaScan system for detection of proximal caries lesions of known size. *Oral Surg Oral Med Oral Pathol Oral*

Radiol Endod 2009; **107**: 116–21. doi: https://doi.org/10.1016/j.tripleo.2008.09.031
13. de Azevedo Vaz SL, Neves FS, Figueiredo EP, Haiter-Neto F, Campos PS. Accuracy of enhancement filters in measuring *in vitro* peri-implant bone level. *Clin Oral Implants Res* 2013; **24**: 1074–7. doi: https://doi.org/10.1111/j.1600-0501.2012.02511.x
14. Hadley DL, Replogle KJ, Kirkam JC, Best AM. A comparison of five radiographic systems to D-speed film in the detection of artificial bone lesions. *J Endod* 2008; **34**: 1111–14. doi: https://doi.org/10.1016/j.joen.2008.06.018
15. Wenzel A, Kirkevang LL. Students' attitudes to digital radiography and measurement accuracy of two digital systems in connection with root canal treatment. *Eur J Dent Educ* 2004; **8**: 167–71. doi: https://doi.org/10.1111/j.1600-0579.2004.00347.x
16. Park SH, Goo JM, Jo CH. Receiver operating characteristic (ROC) curve: practical review for radiologists. *Korean J Radiol* 2004; **5**: 11–18. doi: https://doi.org/10.3348/kjr.2004.5.1.11
17. Schweitzer DM, Berg RW. A digital radiographic artifact: a clinical report. *J Prosthet Dent* 2010; **103**: 326–9. doi: https://doi.org/10.1016/S0022-3913(10)00082-X
18. Dave M, Davies J, Wilson R, Palmer R. A comparison of cone beam computed tomography and conventional periapical radiography at detecting peri-implant bone defects. *Clin Oral Implants Res* 2013; **24**: 671–8. doi: https://doi.org/10.1111/j.1600-0501.2012.02473.x